

The Mechanical and Biological Performance of Photopolymerized Gelatin-Based Hydrogels as a Function of the Reaction Media

Regina Pamplona, Sandra González-Lana, Pilar Romero, Ignacio Ochoa, Rafael Martín-Rapún,* and Carlos Sánchez-Somolinos*


From the first experiments with biomaterials to mimic tissue properties, the mechanical and biochemical characterization has evolved extensively. Several properties can be described, however, what should be essential is to conduct a proper and physiologically relevant characterization. Herein, the influence of the reaction media (RM) and swelling media (SM)—phosphate buffered saline (PBS) and Dulbecco's modified Eagle's medium (DMEM) with two different glucose concentrations—is described in gelatin methacrylamide (GelMA) hydrogel mechanics and in the biological behavior of two tumoral cell lines (Caco-2 and HCT-116). All scaffolds are UV-photocrosslinked under identical conditions and evaluated for mass swelling ratio and stiffness. The results indicate that stiffness is highly susceptible to the RM, but not to the SM. Additionally, PBS-prepared hydrogels exhibited a higher photopolymerization degree according to high resolution magic-angle spinning (HR-MAS) NMR. These findings correlate with the biological response of Caco-2 and HCT-116 cells seeded on the substrates, which demonstrated flatter morphologies on stiffer hydrogels. Overall, cell viability and proliferation are excellent for both cell lines, and Caco-2 cells displayed a characteristic apical-basal polarization based on F-actin/Nuclei fluorescence images. These characterization experiments highlight the importance of conducting mechanical testing of biomaterials in the same medium as cell culture.

1. Introduction

Cells are surrounded by a water-swollen network mainly composed of proteins and polysaccharides which is under constant remodeling: the extracellular matrix (ECM). It is known that cells and the native ECM exist in dynamic reciprocity and consequently, changes in its structure and composition mediate biological processes such as cell adhesion, migration, differentiation and proliferation, as well as pathogenesis of diseases such as cancer.^[1–3] A good comprehension of how cell and ECM interact can lead to a better disease understanding and eventually to more efficient target therapeutic treatments. It is therefore essential to count with biomaterials that provide suitable models offering this tailored interaction with biological entities. In particular, hydrogels, polymeric networks that become hydrated in aqueous media, are being used as artificial matrices trying to mimic the ECM.^[4,5] It is nowadays well-known that not only the biochemical features of the ECM but also local physical properties such as stiffness play a key role in the cell biological processes.^[6] Hence, it is imperative mimicking not only the biochemistry of

R. Pamplona, P. Romero, R. Martín-Rapún
Aragón Institute of Nanoscience and Materials (INMA), CSIC-University of Zaragoza
Department of Organic Chemistry
C/ Pedro Cerbuna 12, Zaragoza 50009, Spain
E-mail: rmartin@unizar.es

S. González-Lana
BEONCHIP S.L., CEMINEM
Campus Río Ebro. C/ Mariano Esquillor Gómez s/n
Zaragoza 50018, Spain
S. González-Lana, I. Ochoa
Tissue Microenvironment (TME) Lab, Aragón Institute of Engineering Research (I3A)
University of Zaragoza
C/ Mariano Esquillor s/n, Zaragoza 500018, Spain
I. Ochoa, R. Martín-Rapún, C. Sánchez-Somolinos
CIBER in Bioengineering
Biomaterials and Nanomedicine (CIBER-BBN)
Madrid, Spain
E-mail: carlos.s@csic.es

 The ORCID identification number(s) for the author(s) of this article can be found under <https://doi.org/10.1002/mabi.202300227>

© 2023 The Authors. Macromolecular Bioscience published by Wiley-VCH GmbH. This is an open access article under the terms of the Creative Commons Attribution-NonCommercial License, which permits use, distribution and reproduction in any medium, provided the original work is properly cited and is not used for commercial purposes.

DOI: 10.1002/mabi.202300227

the matrix but also the ECM mechanics which has turned out to be a challenging but essential step in this research area.

Since the first derivatization of gelatin into gelatin methacrylamide (GelMA),^[7] GelMA-based materials have witnessed a progressively increased use in biomedical applications due to its biocompatibility and ease of manipulation. Indeed, GelMA hydrogels have been ubiquitously applied in the emulation of mechanical and biochemical properties in bone,^[8] stroma,^[9] adipose^[10] and epidermal^[11] tissue engineering, among others. As for the network crosslinking mechanism, free radical photopolymerization is one of the most broadly studied methods to fabricate hydrogels with controlled polymeric architecture owing to its efficiency, simplicity and robustness.^[12] The large spatio-temporal control of the photopolymerization reaction enables also an accurate control of the hydrogel properties with high resolution.^[13] Besides, an easy- and fine-tuning of the mechanical properties is possible thanks to this control of the photopolymerization conditions, which has a large impact in its biological performance.^[10,14–16] In particular, stiffness is a crucial material parameter that influences cellular behavior. According to Daniele et al., a higher spreading of adherent cells was observed with increasing stiffness of GelMA-based hydrogels.^[17] In a similar way, we have also recently reported changes in the villus-like intestinal structures formed by Caco-2 cells when seeded on GelMA-based scaffolds. The substrate stiffness affected the polarization of cells displaying a different organization on hydrogels that mimicked the physiological tissue in contrast to stiffer hydrogels simulating tumoral stages.^[16]

In the same work, remarkably, we found that GelMA-based hydrogels exhibited significantly different properties in terms of gel fraction, mass swelling ratio and stiffness depending on the aqueous media used for hydrogel photopolymerization while keeping the rest of curing conditions the same. In particular, focusing in mechanical properties, GelMA hydrogels showed up to three-times lower Young's Moduli when prepared in Dulbecco's modified Eagle's Medium (DMEM) than their analogs prepared in phosphate-buffered saline (PBS).^[16] Notably, scarce reports about mechanical characterization of hydrogels prepared in different cell culture media are found in literature. In polysaccharide-based bioscaffolds undergoing physical crosslinking,^[18] preparations in DMEM yielded superior mechanical properties resulting from a higher concentration of Ca²⁺ ions in the media. In addition, Gupta and coworkers also reported that the elastic modulus for physically crosslinked gelatin hydrogels was significantly lower when prepared in DMEM compared to PBS but more stable over time.^[19] Recently, the influence of the cell culture media on the photopolymerization of synthetic hydrogels

has been explored by Monfared et al. who studied the interfering mechanisms and effects of cell culture media on the photocuring of acrylamide- or polyethylene glycol (PEG) diacrylate-based polymers.^[20]

At this point, it is of primal importance to recall that the nutritional environment required for every cell line frequently differs in composition and pH.^[21] The metabolism of cultured cells is influenced by the nutrient and growth factors content^[22] that is why over the years, optimal cell culture media have been reported for different cell lines. Since in cell culture systems, biological performance of cells depends on the mechanical properties of bioscaffolds which are affected by the media used during fabrication,^[16] it is of great importance to gain knowledge on the influence of reaction cell culture media on the mechanical and biological performance of photopolymerized hydrogels.

In this paper we perform an in-depth study of the mechanical and biological performance of GelMA hydrogels prepared and swollen in different aqueous media. We have prepared these hydrogels by photopolymerization under the same irradiation conditions but using different media, namely PBS and DMEM with two different glucose concentrations. The hydrogels are then swollen in the media used later for the cell-seeding of the two tumoral cell lines (Caco-2 and HCT-116). Nanoindentation is selected as the method to characterize the elastic modulus of the different hydrogels as this technique explores the material at a similar length scale as the cells do when they are seeded on the surface. In addition, the biological behavior of these bioscaffolds was investigated through the analysis of cell viability, adhesion and proliferation on the hydrogel surface. The relation between the reaction cell culture media used for photopolymerization and the mechanical properties and the biological performance is discussed.

2. Experimental Section

2.1. Materials

Methacrylated gelatin was purchased from Advanced Biomatrix (PhotoGel a trademark of Advanced Biomatrix, catalog #5208). 3-(Trimethylsilyl)propionic-2,2,3,3-d₄ acid sodium salt (TMSP), and photoinitiator 2-hydroxy-4'-(2-hydroxyethoxy)-2-methylpropiophenone, also known as Irgacure 2959 (I2959), were obtained from Sigma Aldrich. Methanol was purchased from PanReac AppliChem ITW Reagents. Deuterium oxide was obtained from Eurisotop. Poly(dimethylsiloxane) (PDMS) elastomer was prepared from Sylgard-184 (Dow Corning). Glass coverslips (thickness: 0.16 mm) for F-actin/Nuclei staining visualization were supplied by Marienfeld GmbH. Phosphate-buffered saline (PBS) pH 7.4, high glucose Dulbecco's modified eagle's medium (DMEM) without Phenol red, Advanced DMEM, DMEM No glucose without Phenol red, Glutamax, Penicillin/Streptomycin (10000 U mL⁻¹) and non-essential amino acids (10X) were purchased from Gibco, Life Technologies. Fetal bovine serum (FBS), D-Glucose, trypsin, Calcein AM (CAM) and propidium iodide (PI) were purchased from Sigma-Aldrich. Hoechst 33342 was obtained from ThermoFisher Scientific. 4% Paraformaldehyde (PFA) was purchased from VWR. Phalloidin-Tetramethylrhodamine B isothiocyanate (TRITC) was supplied by Merck and Mowiol 4–88 reagent was purchased from

I. Ochoa
Institute for Health Research Aragón (IIS Aragón)
Paseo de Isabel La Católica 1–3, Zaragoza 50009, Spain
R. Martín-Rapún
Departamento de Química Orgánica, Facultad de Ciencias
University of Zaragoza
C/ Pedro Cerbuna 12, Zaragoza 50009, Spain
C. Sánchez-Somolinos
Aragón Institute of Nanoscience and Materials (INMA), CSIC-University of Zaragoza
Department of Condensed Matter Physics (Faculty of Science)
C/ Pedro Cerbuna 12, Zaragoza 50009, Spain

CalBiochem. All purchased materials were used without further purification.

2.2. NMR Spectroscopy

All NMR spectra were recorded at room temperature (RT) in a Bruker Avance NEO 400 spectrometer equipped with i-BBO probe to acquire spectra in solution and a (^1H , ^{13}C) double resonance 4 mm gradient high resolution magic-angle spinning (HR-MAS) probe to acquire all HR-MAS NMR spectra. Data were processed using Topspin 4.0.9 software.

GelMA macromer sample was prepared at a final concentration of 25 mg mL^{-1} in deuterium oxide. TMSP was used as internal standard (1 mg mL^{-1}).

GelMA hydrogels were freeze dried, swollen in deuterium oxide and chemical shifts were referenced to TMSP (as internal reference). Samples were mechanically stable at the moderate magic angle spinning rate of 4 kHz used in all the HR-MAS experiments. Centrifugation related phenomena created no sample instabilities.

In order to deepen the influence of the culture medium on the degree of polymerization of the hydrogels, quantitative ^1H - ^{13}C -HSQC (Heteronuclear Single Quantum Coherence) experiments were performed using the Bruker hsqcetgpsisp2.2 sequence following the method described by Guerrini's group in the study of heparins.^[23] No water suppression was applied, in order to prevent effects of water suppression onto the signal intensities. ^1H - ^{13}C - HSQC HR-MAS spectra were acquired only for the three types of hydrogels swollen in PBS (prepared in either PBS, Low Glucose DMEM or High Glucose DMEM). The conversion of the methacryl groups in each hydrogel was calculated according to the integration of the signal at ^1H : 5.7 ppm/ ^{13}C : 124.1 ppm assigned to one of the geminal protons $\text{H}_2\text{C} = \text{C}(\text{CH}_3)$ - in methacrylamide. The signal at ^1H : 0.95 ppm/ ^{13}C : 21.05 ppm belonging to non-reactive groups (γ - $\text{CH}_3^{\text{a+b}}$ valine) was used to normalize the integration among the spectra of different materials. Three replicate samples of each condition were tested for all calculations.

$$\text{Methacryl conversion (\%)} = \frac{\int \text{methacryl in hydrogel}}{\int \text{methacryl in PhotoGel}} \times 100 \quad (1)$$

2.3. Hydrogels Preparation

GelMA hydrogels were generated by free radical photopolymerization of the GelMA macromer in aqueous media –PBS, Low Glucose DMEM or High Glucose DMEM– and a photoinitiator. All gelatin-based solutions were prepared at 6% w/v GelMA macromer and 0.1% w/v I2959 as final concentrations either in PBS, Low or High Glucose DMEM. Low Glucose DMEM was prepared by adding D-Glucose to DMEM No glucose up to a final concentration of 1 g L^{-1} .

To ensure complete dissolution, a stock solution of 1% photoinitiator I2959 was prepared in neat methanol according to the supplier's protocol, which has already been reported in bibliography.^[24] Then, GelMA macromer was weighed and the

required amount of I2959 solution was added. To prepare the first type of hydrogels, the hydrogel precursor mixture was next dissolved in PBS while protected from light and incubated at 37°C for 1 h. Two different hydrogel geometries were fabricated for the following experiments. On one hand for swelling and compression tests, cylindrical hydrogels ($D = 6 \text{ mm}$, thickness = 3 mm) were prepared by pouring $130 \mu\text{L}$ of GelMA hydrogel precursor into PDMS molds as described in our previous work.^[16] On the other hand, disc-shaped hydrogels ($D = 10 \text{ mm}$, thickness = 1 mm) were fabricated for AFM experiments. These thinner samples were prepared by adding $120 \mu\text{L}$ of mixture into PDMS molds mounted on top of glass slides. Hydrogels were then incubated at RT for 20 min whilst physical gelation took place. Finally, hydrogels were exposed for 150 s to UV light ($320\text{--}390 \text{ nm}$, 10 mW cm^{-2}) using an OmniCure S2000 UV Lamp, yielding the final photopolymerized hydrogels.

To prepare hydrogels in culture medium the same protocol was followed, substituting PBS for Low or High Glucose DMEM. Since Phenol red may cause unwanted potential effects during photopolymerization such as UV light absorption and attenuation,^[20] Phenol red-free culture media was employed for the hydrogels mixture step. Thus, hydrogels were prepared in Low or High Glucose DMEM supplemented with 1% Penicillin/Streptomycin and 1% v/v of non-essential amino acids (supplemented DMEM media without FBS will be named as D0 and DG0 for Low and High Glucose, respectively). All processes were performed under sterile conditions.

The experiments described in the following sections of hydrogels characterization were performed with seven types of samples, varying the reaction media (RM) and the swelling media (SM). Hydrogels prepared in PBS and swollen in PBS, D0, or DG0 will be named as PBS-PBS, PBS-D0, or PBS-DG0 respectively. Hydrogels prepared in D0 and swollen in PBS or D0 will be named as D0-PBS and D0-D0 respectively. Finally, hydrogels prepared in DG0 and swollen in PBS or DG0 will be named as DG0-PBS or DG0-DG0 respectively.

2.4. Hydrogels Characterization

2.4.1. Swelling Behavior

The swelling ratio is determined by the amount of aqueous medium that can be absorbed by a polymer. To calculate this parameter, photopolymerized hydrogels were first incubated in either PBS, D0 or DG0 at 37°C for 24 h under sterile conditions. Next, the excess of aqueous solution was blotted with a KimWipe paper and scaffolds were weighed (W_s). At last, the dry mass of hydrogels was obtained after freezing them in liquid nitrogen, lyophilizing overnight and weighing again (W_d). Mass swelling ratio (g/g) was defined as:

$$\text{Mass swelling ratio (g/g)} = \frac{W_s}{W_d} \quad (2)$$

Three replicate samples of each condition were tested for all calculations.

2.4.2. Mechanical Testing: Atomic Force Spectroscopy

Atomic Force Spectroscopy (AFM) measurements were performed in contact mode using a NanoWizard 3 AFM module (JPK Instruments AG, Germany) equipped with an optical inverted microscope (Nikon-Eclipse). Nanoindentation experiments were performed with qp-BioAC-CB1 probes (Nanosensors, Switzerland) with a nominal spring constant of 0.3 N m^{-1} . As recommended, calibration of the cantilever was previously performed to mechanical testing. The specific spring constant was measured using the thermal noise method before each experiment. Measurements were performed in the same medium as in which the hydrogel was swollen -either PBS, D0, or DG0- at 37°C with the aid of a petri dish heater (JPK Instruments AG, Germany). Since disc-shaped hydrogels would float if directly immersed in aqueous media hence hampering nanoindentation, they were directly cured onto a glass substrate in order to weigh enough to keep them immobile. The easy-handling ensemble was incubated in the corresponding aqueous media at 37°C for 24 h and then placed inside the petri dish filled with tempered aqueous media. Force-distance curves were recorded at a scan rate of $2 \mu\text{m s}^{-1}$, up to a force setpoint of 1 nN. Force mappings of 8×8 pixel resolution were acquired over a $10 \times 10 \mu\text{m}$ area and three to four maps were recorded per sample. AFM software (JPK SPM Desktop – Nanowizard) was used to calculate Young's Moduli by fitting the collected force curves to Hertz model approximating the tip as a 15° cone. Three samples of each condition were tested for calculations of means and standard deviations.

2.4.3. Mechanical Testing: Unconfined Compression Testing

The compressive properties of the hydrogels were measured using a 5548 microtester (Instron, Norwood, MA USA) with a 5N load cell. Hydrogels were prepared 1 day before testing and incubated at 37°C in the corresponding SM. Cylindrical samples were immersed in the same media used for each swelling condition tempered at 37°C and the compression rate applied was 1 mm min^{-1} . Compressive Young's Moduli were calculated from the slope of the stress-strain curve at the linear region 10–15% strain. For each GelMA hydrogel type, three replicas were tested for all calculations.

2.5. Cell Culture

Caco-2 cells and HCT-116 were cultured in flasks in Advanced DMEM supplemented with 10% v/v FBS and 1% Penicillin/Streptomycin (DG10). DG10 for Caco-2 cells also contained 1% v/v of non-essential amino acids. Cells were maintained at 37°C in a humidified incubator with 5% CO_2 (standard conditions), exchanging the medium every 2–3 days until they reached 90% confluence. For cell culture experiments, two types of hydrogels were prepared depending on the reaction aqueous media: PBS or DG0. Scaffold geometry was the same as in AFM testing and PDMS molds with 10 mm diameter and 1 mm thick were used to fabricate GelMA hydrogels. After the 150s UV period, both hydrogels were transferred to 24-well plates and incubated

in DG0 at 37°C until cell seeding. Caco-2 and HCT-116 cells were trypsinized, counted and re-suspended in DG10 at a density of 2×10^6 cells/mL. After 24 h of hydrogel swelling, cell-seeding was performed on top of the 6% w/v GelMA-150 substrates to create the in vitro model. 24 h later, cell-seeded hydrogels were transferred to new 24-well plates and the experiment was maintained for 14 days under standard conditions refreshing the DG10 every 2–3 days. Three hydrogels were cell-seeded for each condition of RM and cell type.

2.5.1. Cell Viability

Cell viability was quantified by Live/Dead staining after Caco-2 and HCT-116 cells were cultured for 1, 7, and 14 days. Cell-seeded hydrogel discs were incubated with DG10 containing CAM ($2 \mu\text{g mL}^{-1}$) and PI ($4 \mu\text{g mL}^{-1}$) for 25 min under standard culture conditions. After this incubation period and in order to acquire defined fluorescence images, hydrogels were transferred to new 24-well plates with the cell layer downward. Then, hydrogels were covered with DG10 and viability was evaluated using an inverted fluorescence microscope (Leica DMi8). Subsequent fluorescence image analysis was performed using ImageJ software and cell viability was quantified by manual threshold.

2.5.2. Phalloidin Staining & Visualization of Actin

After 1, 7, and 14 days of culture on the GelMA-based hydrogels, cell-seeded samples were rinsed with PBS three times and fixed with 4% PFA for 20 min at RT. Following three new washes in PBS, F-actin and cell nuclei were stained by incubating with Phalloidin-TRITC ($2 \mu\text{g mL}^{-1}$) and Hoechst 33342 ($\approx 40 \mu\text{g mL}^{-1}$) for 60 min at RT while protected from light. After rinsing three times with PBS, hydrogels were deposited with the cell layer downward in a glass coverslip coated with Mowiol. Confocal images were obtained with a 40X oil-immersion objective (Nikon Ti-E coupled to a C1 modular confocal microscope).

2.5.3. Scanning Electron Microscopy (SEM) Imaging of Cell-Seeded Hydrogels

Just as described in the previous section, fixation with PFA was the first step in samples preparation for SEM imaging. Next, dehydration through a graded ethanol series (30-50-70-90-96-100-100-100%) was performed with cell-seeded hydrogels (day 1, 7, and 14) for 10 min each and drying at RT overnight. At last, hydrogels were placed on stubs using conductive carbon tape, coated with a 14 nm sputtered palladium layer and examined under a scanning-electron microscope (CSEM-FEG Inspect 50, FEI). The acceleration voltage was set to 10 kV and spot size 3.

2.6. Data Analysis and Statistics

All results are reported as mean \pm standard deviation (SD). OriginPro 2020 software (OriginLab) was used in graphs plotting and statistical analysis. Before significance testing, normality through

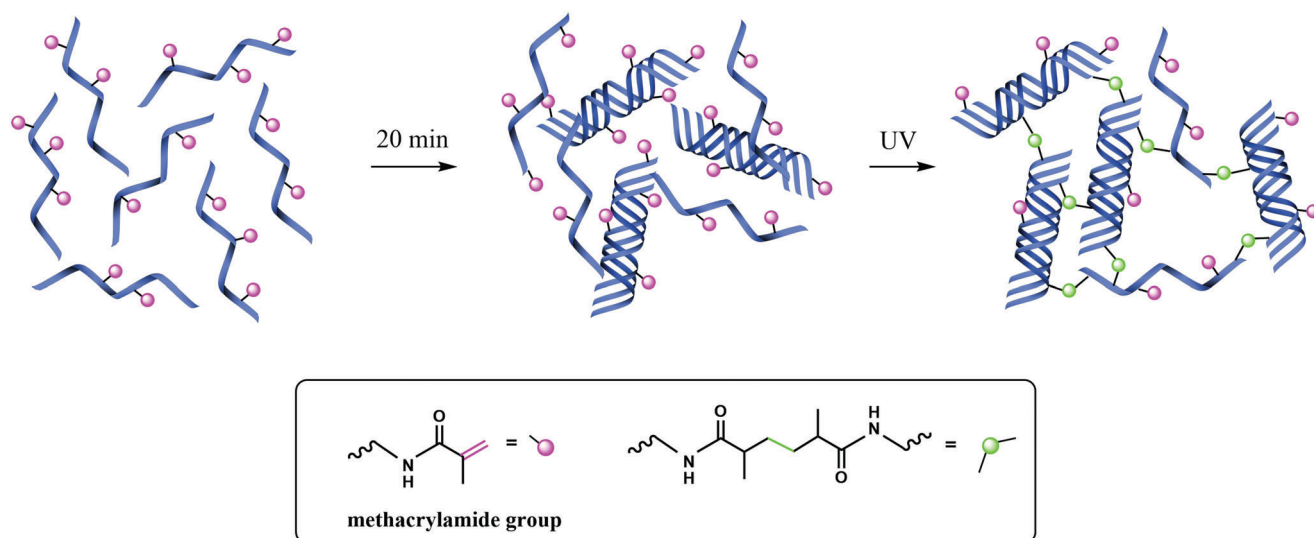


Figure 1. Photochemical crosslinking takes place after physical gelation at RT in GelMA-150 hydrogels.

Shapiro-Wilk test and equality of variances between datasets were studied. Significant differences ($p < 0.05$) were assessed with Student's t-tests and one-way ANOVAs with Tukey's post hoc tests. In Figure 2 and Figure 3, statistical significance of differences was determined at $p < 0.0001$.

3. Results and Discussion

3.1. Preparation and Characterization of Cell-Free Hydrogels

It is worth noting that mechanical characterization of hydrogels is performed in PBS in the vast majority of articles. However, for biological studies in which cells are involved, these are suitable analyses on the condition that subsequent cell experiments are also carried out in PBS. Nevertheless, the absence of nutrient content in this buffer has detrimental effect on the viability of certain cell lines when embedded in hydrogels prepared in PBS,^[25] making necessary to work with cell culture media. In our previous work on different strategies to crosslink GelMA macromer and their impact in the mechanical and biological properties of the bioscaffolds, we also observed the RM had an impact on the mechanical properties.^[16] Therefore, we wanted to carry on and gain insight in these differences by performing a characterization research including also the biological performance of the scaffolds. Thus, GelMA hydrogel precursors in different RM were prepared with commercially available methacrylated gelatin PhotoGel at final concentrations of 0.1% I2959 and 6% GelMA macromer according to their already demonstrated good cell viability. The irradiation time chosen was 150 s (GelMA-150 hydrogels) due to several reasons. First of all, the high stiffness described for those scaffolds represents a good reference value to appreciate significant differences during the comparison with other scaffolds while being in the range of colorectal tumor tissues.^[26] In addition, GelMA-150 hydrogels exhibited an excellent cell adhesion after 24 h of cell seeding, as well as good cell viability and proliferation over a long culture period (14 d).

Table 1. Types of GelMA-150 hydrogels varying reaction and swelling media.

Reaction media (RM)							
PBS			D0		DG0		
Swelling media (SM)							
PBS		D0	DG0	PBS	D0	PBS	DG0
Hydrogels' nomenclature							
PBS-PBS		PBS-D0	PBS-DG0	D0-PBS	D0-D0	DG0-PBS	DG0-DG0

The first step in hydrogel preparation was pouring the warm GelMA hydrogel precursors into PDMS molds (see details in Experimental Section). Samples were then incubated for 20 min at RT protected from light before photoirradiation. Meanwhile, a physical gel is formed due to hydrogen bonding between GelMA macromer chains, changing the geometrical disposition from random coil to triple helix (**Figure 1**).^[27] According to Van Hoorick et al.,^[28] mechanically superior materials are obtained when physical gelation takes place prior crosslinking. For this reason, UV irradiation was applied after the 20 min of incubation period in order to achieve stiffer covalently crosslinked networks.

Thus, the formulation containing GelMA macromer and the photoinitiator was exposed to actinic light and the network formation followed a chain-growth mechanism. A large number of works in the literature have thoroughly described and investigated this light-induced procedure owing to its almost unlimited photopolymerization possibilities.^[29–31]

As for the buffers, we decided to establish a small set of aqueous media (PBS, D0, and DG0) to test the possible differences that they may generate in hydrogels outcome. Mechanical and biological properties of bioscaffolds could be influenced by the RM but also by the SM, that is why we prepared the 7 types of hydrogels according to **Table 1**, that were systematically named following the nomenclature RM-SM, incorporating in this name the reaction and swelling media respectively. PBS is the most

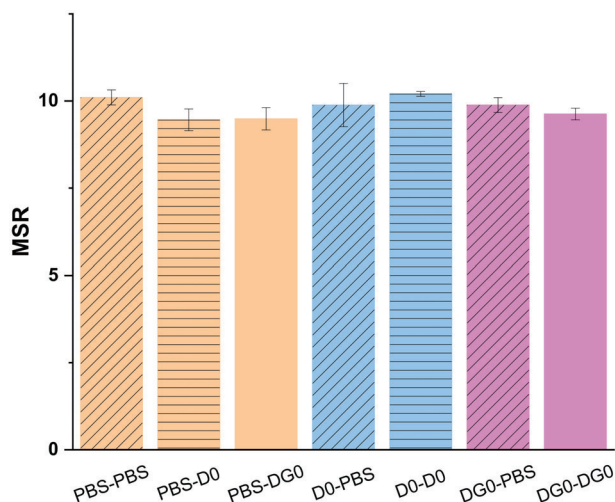


Figure 2. Mass swelling ratio MSR data for GelMA-150 hydrogels prepared and swollen in either PBS, D0, or DG0. Error bars SD. Statistics between datasets yielded non-significant differences in all cases.

extensively used buffer for preparation and characterization of bioscaffolds. It is a pH 7.4 multicomponent electrolyte, while DMEM media are additionally supplemented with other inorganic and organic salts, vitamins and glucose. D0 was the original formula containing 1 g L^{-1} of glucose but a further modification with 4.5 g L^{-1} (DG0) proved to be optimal for culture of certain cell types.^[32,33] Thus, the comparison between PBS and DMEM as both RM and SM, will evidence the effect of biologically active substances in the final mechanical and biological properties of the hydrogels and more specifically, the influence of glucose concentration will be studied during the analysis of D0 and DG0 hydrogels results. Since the glucose content in DMEM (Low or High) is a well-established parameter for each specific cell line, combinations between D0 and DG0 (D0-DG0 and DG0-D0) were not physiologically relevant, hence discarded for the present study.

3.1.1. Mass Swelling Ratio

The mass swelling ratio (MSR) is an important physical property that influences cell behavior and is related to the hydrogel mesh size.^[34] The extent of crosslinking and the macromer concentration have a strong influence on MSR.^[17] In fact, it has been widely reported that the less crosslinked a network is, the higher its mesh size and swelling ratio.

According to **Figure 2**, the swollen weight was approximately ten times higher than the dry weight, in all of the seven types of hydrogels. These results might indicate that all hydrogels achieved a similar photopolymerization degree, regardless the aqueous media used for mixture preparation.

3.1.2. AFM

As our efforts in these materials are focused on in vitro studies, we have selected to characterize the mechanic microenvironment

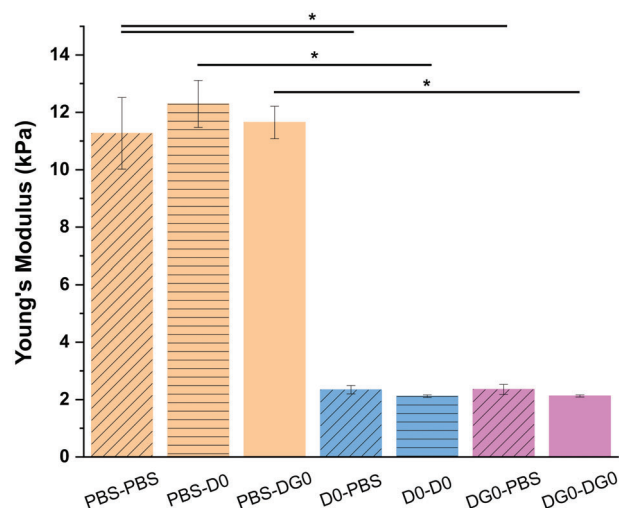


Figure 3. Young's Moduli obtained by AFM of GelMA-150 hydrogels prepared and swollen in either PBS, D0, or DG0. Error bars SD. Note: * $p < 0.0001$. Non-significant differences are not drawn in the graph.

of the surface where cells were cultured. Local nanoindentations in the hydrogels were performed with an AFM equipment. The mechanical properties of the 7 types of hydrogels were measured at 37°C while immersed in the same aqueous media as the one used for swelling.

First of all, a prominent drop in stiffness was evident for DMEM-prepared hydrogels –both D0 and DG0– compared to their PBS analogs (**Figure 3**). PBS-prepared hydrogels exhibited Young's Moduli near 12 kPa, regardless the medium used for swelling, while scaffolds prepared in D0 and DG0 showed values six times lower, being $\approx 2 \text{ kPa}$ –with no significant differences between D0 and DG0. Taken all together, we could conclude that the RM has a marked effect on mechanical properties measured at the surface that could be ascribed to the radical photopolymerization during network formation. To date, there are nearly no reports on this respect being remarkable the work focused on the effect of aqueous media on photopolymerizations by Monfared et al.^[20] These authors investigated the radical polymerization of *N,N*-dimethylacrylamide (DMA) using UV light and I2959 as the photoinitiator. They performed an exhaustive mechanical characterization of PDMA, however no biological studies in cell culture were reported. The authors concluded that media had a radical quenching effect and inhibited the start of photopolymerization. Focusing on the specific molecules with radical scavenging ability, Monfared and coworkers claimed that the induction time before polymerization started could partially correspond to the chain transfer effect of vitamin B6 and BSA. Interestingly, they also proved that thiol-containing amino acids present in media hardly influenced photopolymerization. In the present case, in addition to the aforementioned statements, amine groups present in amino acids in the culture medium might also be involved in side reactions, especially glutamine, which is in a much higher concentration than the other amino acids. We hypothesize about the reaction of amine groups with methacrylic groups through a conjugated nucleophilic addition occurring during the photoirradiation step and consequently diminishing crosslinking in DMEM-prepared hydrogels.

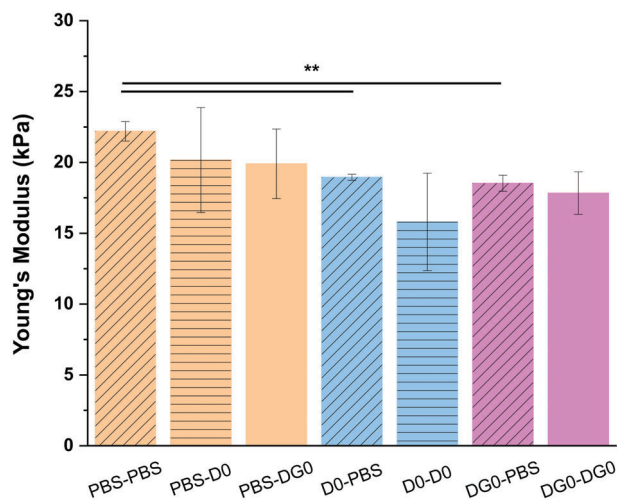


Figure 4. Stiffness results obtained by compression testing for GelMA-150 hydrogels prepared and swollen in either PBS, D0, or DG0. Error bars SD. Note: ** $p < 0.01$.

Finally, according to Figure 3, neither the swelling aqueous media (SM) nor the glucose concentration had influence on the stiffness.

3.1.3. Compression Tests

We also evaluated the stiffness of the hydrogels with compression measurements (Figure 4). With this technique we observed smaller differences among the materials -Young's Moduli were all in the range of 15–22 kPa-, but still the hydrogels prepared in PBS exhibited higher Young's moduli than hydrogels prepared in culture media.

Unlike AFM characterization in which each nanoindentation measurement evaluates the stiffness of the sample surface, during compression analysis the entire hydrogel is tested. This would explain a better agreement of compression results with MSR experiments, a property which also averages the whole scaffold. On the other hand, AFM results could correlate better with the biological response of cells seeded on the hydrogel surface.

3.1.4. HR-MAS NMR

Aiming to quantify the extent of methacryl conversion in hydrogels, HR-MAS NMR spectroscopy was used. As already confirmed by stiffness measurements –both compression and AFM–, the swelling aqueous media had scarce influence on photopolymerization. For this reason, we decided to chemically characterize the three types of hydrogel swollen in PBS, but prepared with different media: PBS, D0, and DG0. All three samples were freeze dried and swollen with deuterium oxide.

^1H HR-MAS NMR has already been used for the quantitative determination of the chemical crosslinking,^[35,36] but the enhanced signal dispersion of 2D-NMR HSQC improves spectral resolution and facilitates structural identification. The choice of the appropriate pulse sequence has allowed us both the resolution and the quantification of the signals. On the

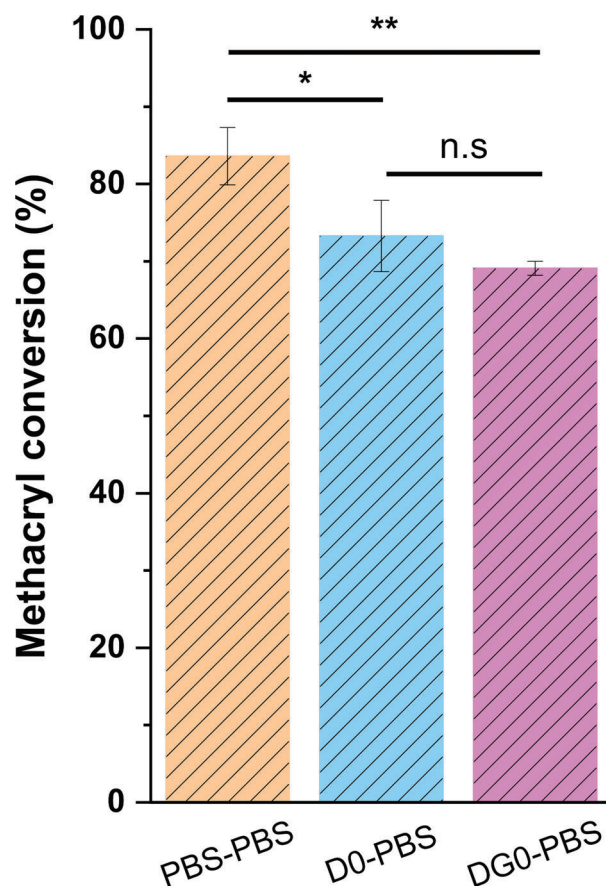


Figure 5. Methacryl conversion for the three types of GelMA-150 hydrogels swollen in PBS. Error bars SD. Note: ** $p < 0.01$, * $p < 0.05$.

other hand, although ^1H - ^{13}C -HSQC experiments with gelatin and its derivatives have been described,^[37] to the best of our knowledge, this is the first time that ^1H - ^{13}C -HSQC HR-MAS experiments of gel-phase photopolymerized GelMA have been reported.

The decrease of signal belonging to the vinyl protons was quantified by integration of the acquired ^1H - ^{13}C -HSQC spectra and the methacryl conversion was calculated (signal at ^1H : 5.7 ppm/ ^{13}C : 124.1 ppm). The same trend can be seen in the decrease in the integral of the signal at ^1H : 1.94 ppm/ ^{13}C : 20.8 ppm corresponding to methyl of metacrylamide and methacrylate groups. (Figures S1 and S2, Supporting Information).

According to Figure 5, the RM has a marked effect on the photopolymerization. Thus, the methacryl conversion was significantly higher in PBS (83.6%) than in D0 (73.3%) and DG0 (69.1%). These results mean that in PBS, a higher number of methacryl groups react during UV irradiation. Since termination reaction can also occur with methacryl groups, we cannot assure that all methacryl groups react to yield new network bonds, however it is expected that the vast majority of them contribute to the network crosslinking. On the other hand, precisely according to these methacryl conversion results, the lower degree of crosslinking–hence lower mechanical properties–in DMEM-prepared hydrogels cannot be due to

parasite reactions of methylene double bonds (such as conjugated nucleophilic addition) but to other factors as explained below.

Among the plethora of biomolecules contained in DMEM, ascorbic acid phosphate is one of the vitamins present. Due to its longer stability, ascorbic acid phosphate progressively substituted ascorbic acid in cell culture media and it is a well-described antioxidant agent.^[38] At physiological pH, it specially exists as an ascorbate anion which primarily reacts with other radicals. As determined experimentally, the photopolymerization degree in DMEM resulted lower than in PBS and one of the possible causes of interference could be the role of this ascorbate anion as a terminator of free radical chain reactions.^[39]

In addition, we also hypothesize about the steric hindrance generated by the biomolecules present in DMEM. As a consequence of their volume and the flow across the hydrogel, methacryl radicals could be hidden from each other, yielding a decreased extent of crosslinking.

3.2. Cell Culture

Besides studying the differences in the chemical and mechanical properties of GelMA-150 hydrogels processed in the different media, going one step further, it is also in the main focus of this paper to investigate how these differences affect the biological behavior in cell culture.

3.2.1. Cell Adhesion and Proliferation

Regarding cell culture assays, the biological behavior of two different cell lines was studied: Caco-2 and HCT-116. It is highly recommended for both cell lines to perform cell culture with High Glucose DMEM, which is why we chose the two substrates swollen in DG0 but prepared in PBS or DG0. Cell seeding was performed on top of PBS-DG0 and DG0-DG0 scaffolds and cell viability was assessed using a CAM/PI staining after 1, 7, and 14 days of cell culture. As shown in **Figure 6A**, Caco-2 cells adhered distinctly onto the two substrates and started to form a flatter layer on PBS-DG0 than in DG0-DG0 hydrogels (10X micrographs are shown in Figure S3, Supporting Information). This flattened morphology observed for PBS-prepared hydrogels was confirmed with the SEM images, as well as the more grouped and stacked distribution of cells when grown on DG0-prepared hydrogels (the corresponding discussion will be addressed in the next section). Furthermore, cell surface coverage was significantly higher for PBS-DG0 hydrogels ($\approx 90\%$) than their DG0-DG0 analogues ($\approx 79\%$), matching with the also higher stiffness of the former scaffolds as measured by AFM (11.6 kPa and ≈ 2.1 kPa, for PBS-DG0 and DG0-DG0 respectively). This finding agrees with the results of DiMarco and coworkers who also found that Caco-2 adhesion was enhanced in stiffer substrates.^[40] As for cell proliferation, at D7, cells had managed to create a monolayer in both conditions with no significant differences with D14 results. According to figure 6C, dead cells stained with PI covered a larger area at D1 (in both conditions) than at D7 and D14. Cell toxicity after 24 h of cell culture might be attributed to the cells that did not adhere to the GelMA

substrates. The progressive detachment of these dead cells after the regular media exchanges and the excellent compatibility of the substrates are responsible for the low cytotoxicity found at D7 and D14 (red areas below 0.1% in both cases).

Similar to Caco-2 response, HCT-116 cells showed an improved adhesion on PBS-DG0 hydrogels ($\approx 65\%$ surface coverage) than DG0-DG0 ($\approx 35\%$ surface coverage), at day 1 (Figure 6D). Besides, cells also proliferated differently over time, exhibiting a higher surface coverage area on PBS-DG0 ($\approx 94\%$) than in DG0-DG0 ($\approx 79\%$) at day 7 (Figure 6B). While HCT-116 cells had almost created a complete monolayer on PBS-prepared substrates, cell proliferation was more pronounced on their DG0 analogs (compared to day 1) but forming clusters. In fact, the green area belonging to alive cells increased 1.4 times at D7 in PBS-DG0 hydrogels and 2.3 times in DG0-DG0 substrates. These proliferation rates are partly related to the initial surface coverage and as expected, the hydrogels less densely colonized at D1 (DG0-DG0) exhibited a higher cell proliferation. As for the different HCT-116 morphology displayed on both substrates, it could be due to the chemical composition and the mechanical properties of the surface. Arginine-glycine-aspartic acid (RGD) binding domains present in GelMA macromer are partly responsible for cell attachment and spreading, being proportionally correlated.^[40,41] Since mass swelling ratio is similar for both conditions, RGD density should also be similar, pointing out that the formation of HCT-116 clusters on DG0-DG0 hydrogels is truly due to the lower stiffness. In addition, and just as explained for Caco-2 cells, the mechanical behavior of the hydrogels is a relevant parameter. Stiffer substrates are known to lead to a higher cell proliferation^[42] and in our case where Young's Moduli sharply rises from 2.1 kPa in DG0-DG0 hydrogels to 11.6 kPa for PBS-DG0, it is not surprising that HCT-116 cells better proliferated on the latter ones. This specific biological response as a function of the hydrogel stiffness highlights how mechanics and biological properties are highly correlated.

Finally, after 14 days of cell culture, both conditions achieved a confluent layer all over the hydrogels surface with similar cell mortality. But in contrast with Caco-2 behavior, HCT-116 dead cells covered a larger area at day 7 and 14 ($> 0.2\%$), than at day 1 ($< 0.1\%$). This higher mortality is related to the cell morphology exhibited on the substrates surface. Caco-2 cells proliferated in a flat and spread manner allowing dead cells to detach and be removed during media exchange. However, since HCT-116 cells formed clusters, dead inner cells could not be detached and PI area kept increasing over time.

Regarding the comparison between the distinct adhesion and growth patterns displayed by the two types of cells, it should be noted that despite having an adherent and epithelial nature both of them, each one possesses a particular morphology when seeded on bidimensional substrates. In general, a flattened morphology was observed in micrographs of Caco-2 cells in agreement with the well-known behavior of these cells to grow as a monolayer^[43] while HCT-116 cells clusters presented heterogeneous shapes and kept on aggregating over time. This experimental result also aligns with the fact that HCT-116 cells usually adopt a spheroid morphology and cell clusters tend to aggregate to form colonies.^[44]

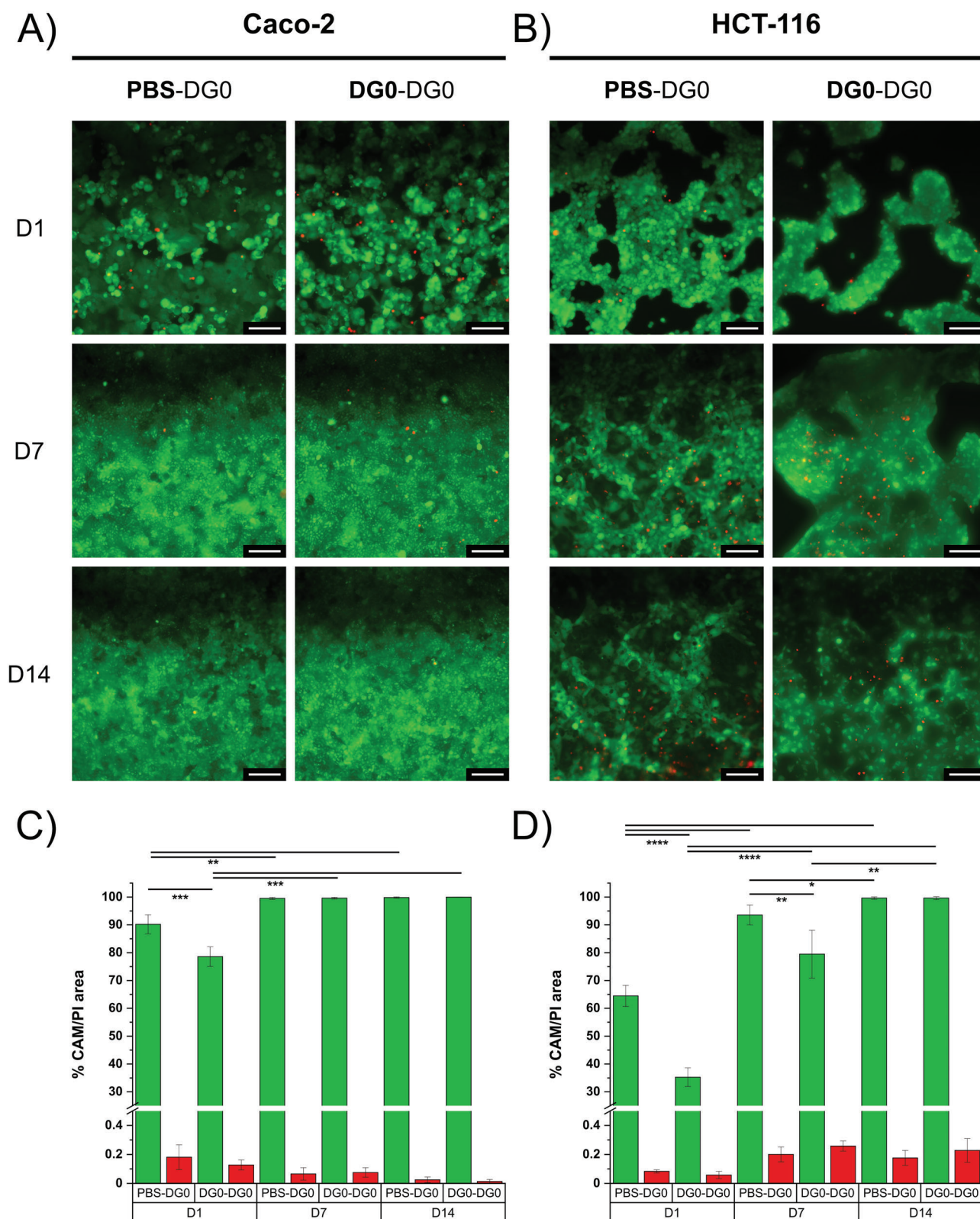


Figure 6. Culture of Caco-2 and HCT-116 cells on GelMA-150 hydrogels over 14 days. A) Live/dead micrographs of Caco-2 and HCT-116 evolution on PBS- and DG0-prepared scaffolds on day 1, day 7, and day 14 of cell culture. The scale bar represents 100 μ m. B) Area percentage of alive CAM (green) and dead PI (red) stained cells from micrographs of Caco-2 and HCT-116 on GelMA-150 scaffolds on day 1, day 7, and day 14 of cell culture. Error bars SD. Note: **** $p < 0.0001$, *** $p < 0.001$, ** $p < 0.01$, * $p < 0.05$.

Caco-2

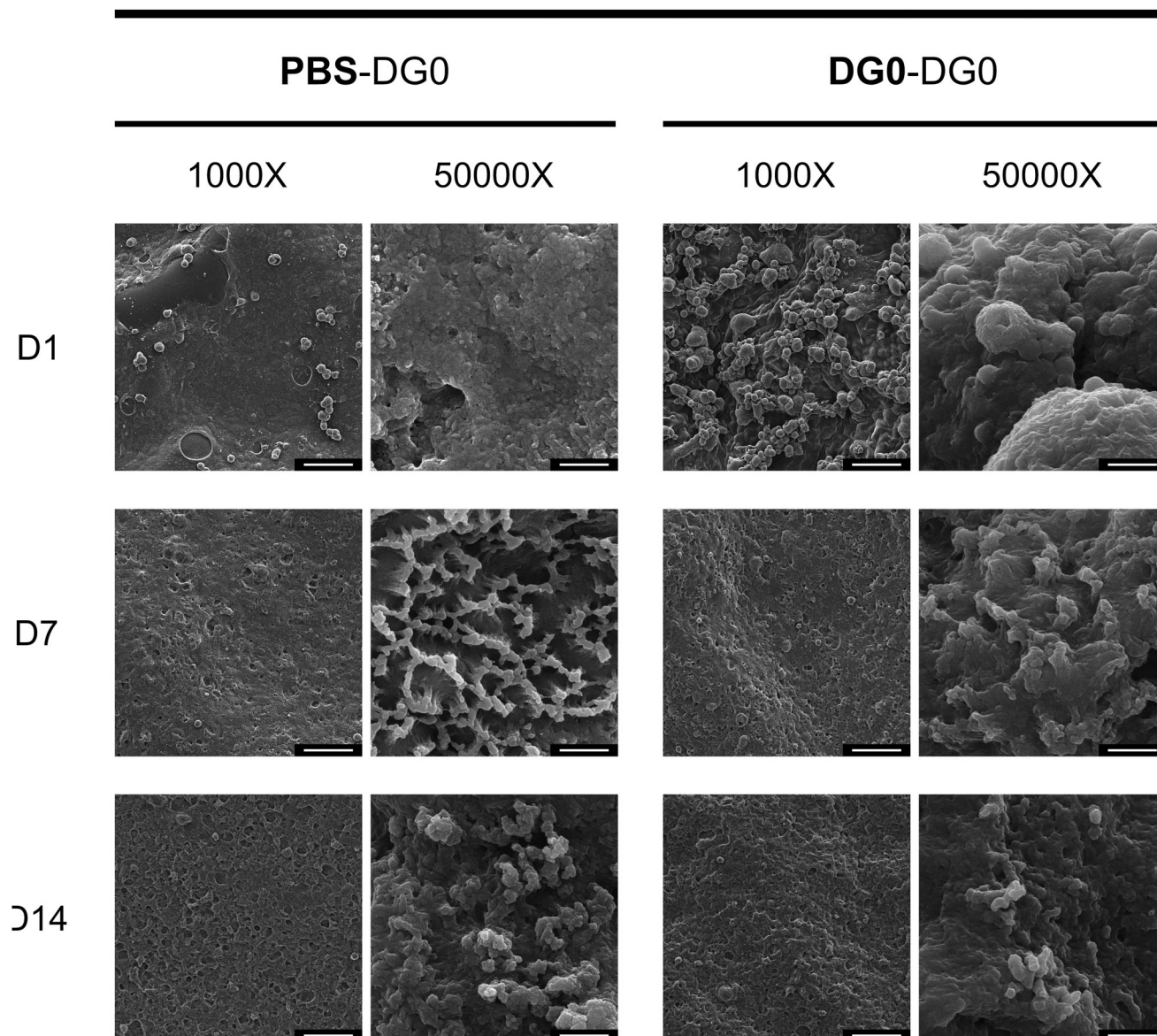


Figure 7. SEM images of Caco-2 cells on PBS- and DG0-prepared scaffolds at days 1, 7, and 14. The scale bar represents 50 μm and 1 μm for 1000 \times and 50000 \times micrographs, respectively.

3.2.2. F-actin/Nuclei Fluorescence Staining and SEM Imaging

SEM micrographs of the cell-seeded hydrogels also confirmed the different morphology adopted by Caco-2 cells depending on the substrate (**Figure 7**). Indeed, Caco-2 cells grew in a flatter layer on PBS-DG0 hydrogels than in DG0-DG0, as already found with fluorescence images at day 1 (**Figure 8**). On PBS-DG0 substrates, a thin monolayer of cells was displayed while on DG0-DG0, cells were heterogeneously grouped forming protrusions and light domes. After 7 days of culture, Caco-2 cells exhibited a noticeable apical-basal polarization in both conditions, however more tightly packed microvilli were observed on PBS-DG0 scaffold,

probably due to its six-times-higher stiffness. At day 14, there was observed a loss in the characteristic organization of Caco-2 cells also in both conditions, probably due to a massive proliferation.

According to **Figure 8**, it was confirmed the different adhesion of Caco-2 cells on the substrates at day 1. On the one hand, cells were attached as a monolayer over PBS-DG0 hydrogels of 35 μm thickness while over DG0-DG0 scaffolds, cells formed protrusions and achieved a layer thickness of 52 μm . **Figure S4** (Supporting Information) shows F-actin/Nuclei fluorescence images of DG0-DG0 scaffolds also at days 7 and 14. At day 7, a marked apical-basal polarization of cells was displayed on

Caco-2

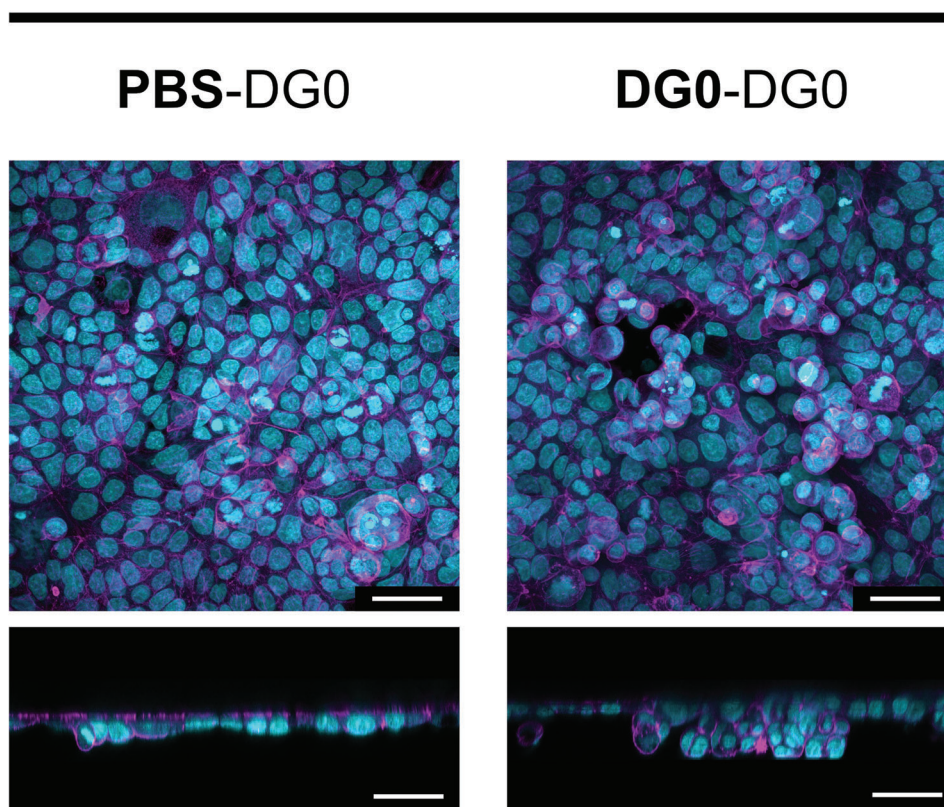


Figure 8. Confocal cross-sectional Z-stack (above) and orthogonal view (below) images of Caco-2 cells on PBS- and DG0-prepared hydrogels at day 1. F-Actin in magenta and nuclei in blue. The scale bar represents 50 μm .

DG0-DG0 hydrogels based on the F-actin brush border. This distribution agrees with SEM micrographs where microvilli were observed. Besides, the cell layer gained thickness up to 57 μm . Interestingly, a flatter cell layer (40 μm) was found at day 14, matching with the massive proliferation shown by SEM pictures as well. It is worth mentioning that despite the thickness decrease, the F-actin brush border was still evident at day 14.

Due to washing and protocol manipulation, HCT-116 cells at day 1 were detached from the two types of substrates suggesting poor initial attachment forces. Neither F-actin/Nuclei fluorescence images nor SEM micrographs were representative enough to study cell morphology at this time point. If HCT-116 cells had not achieved a good adhesion yet on the substrates after 24 h of cell seeding, an early manipulation during PFA fixation protocol might have caused this cell detachment. Regarding day 7 and day 14, HCT-116 also exhibited a more homogeneous and flattened distribution on PBS-DG0 hydrogels than in DG0-DG0, similar to the observed Caco-2 behavior (Figure 9).

F-actin/Nuclei confocal micrographs also confirmed the different cell proliferation depending on the substrate (Figure S5, Supporting Information). At day 7, HCT-116 cells grown on PBS-DG0 hydrogels were displayed as a homogeneous confluent layer

of 70 μm thickness. However, on DG0-DG0 scaffolds, interconnected clusters of cells were found with undulating morphology thereby forming a thicker layer of more than 100 μm . At day 14, cell layer continued growing upward in both conditions, resulting in thicknesses of 90 μm and also more than 100 μm for PBS- and DG0-prepared scaffolds, respectively.

4. Conclusions

The influence of reaction (RM) and swelling media (SM) in GelMA hydrogel mechanics and cell response has been assessed in the present work. On the one hand, swelling behavior is not affected by none of these two factors, however, stiffness results do differ depending on the reaction aqueous media. In all cases, the Young's Moduli obtained for PBS-prepared hydrogels were higher than for their DMEM analogs pointing out a different extent of crosslinking. The existing differences in the photopolymerization degree were confirmed by HR-MAS NMR where methacryl groups conversion was quantitatively measured. This finding agrees with previous research about how biomolecules content in aqueous media interferes with free radical photocrosslinking and sets an essential characterization basis in biomaterials field.

HCT-116

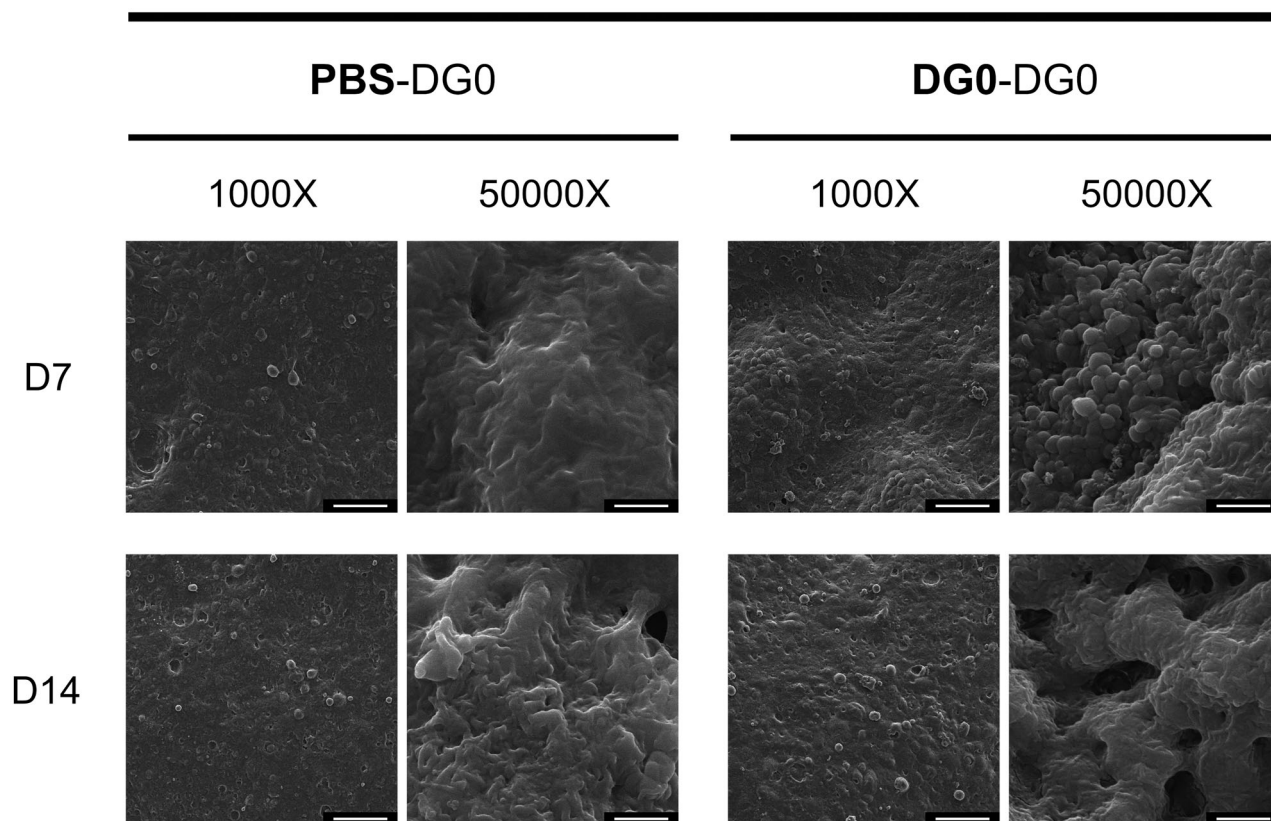


Figure 9. SEM images of HCT-116 cells on PBS- and DG0-prepared scaffolds at days 7 and 14. The scale bar represents 50 μm and 1 μm for 1000 \times and 50000 \times micrographs, respectively.

In addition, stiffness measured through AFM correlated with the biological performance. Caco-2 and HCT-116 cells were grown on GelMA-150 substrates resulting in more spread morphologies, particularly pronounced during the first days of cell culture, when PBS was used as RM, that is, for the stiffer hydrogels. Likewise, cell attachment at D1 was 1.1 and 1.9 times higher in PBS-prepared hydrogels for Caco-2 and HCT-116 cells, respectively. The cell distribution was observed with live/dead and SEM images and further confirmed by quantifying the cell layer thickness in F-actin/Nuclei staining cross-sectional micrographs. Excellent cell viability and proliferation were also found during the in vitro cell culture period for both cell lines. In addition, apical-basal polarization of Caco-2 cells was shown in F-actin/nuclei images, being especially evident at day 7.

These characterization experiments prove the importance of performing mechanical testing on biomaterials samples which have been photopolymerized in the specific same medium that will be used for subsequent cell culture samples, hence establishing highly-valuable guidelines for biomedical research.

Supporting Information

Supporting Information is available from the Wiley Online Library or from the author.

Acknowledgements

The authors acknowledge the use of instrumentation, as well as the technical advice provided by the National Facility ELECMI ICTS, node “Laboratorio de Microscopías Avanzadas (LMA)”, NMR Service of CEQMA (UZ-CSIC), “Servicio General de Apoyo a la Investigación (SAI)”, and ICTS “NANBIOSIS” Unit 13 of the CIBER in Bioengineering, Biomaterials & Nanomedicine (CIBER-BBN) at the University of Zaragoza. This work was funded by MCIN/AEI/ 10.13039/501100011033 and by “ERDF A way of making Europe” through grants PID2020-118485RB-I00, PID2019-109333RB-I00 and PID2021-126132NB-I00, Gobierno de Aragón and “ERDF A way of making Europe” through grant LMP221_21; through the “Fondo Social Europeo” (DGA E15_20R). This research was also supported by CIBER -Consortio Centro de Investigación Biomédica en Red- (CB06/01/00263), Instituto de Salud Carlos III, Ministerio de Ciencia e Innovación. RPC acknowledges Gobierno de Aragón for a predoctoral fellowship (2017-2021). SGL was funded by Spanish MINECO fellowship (DI-17-09585).

Conflict of Interest

The authors declare no conflict of interest.

Author Contributions

The manuscript was written through contributions of all authors. All authors have given approval to the final version of the manuscript.

Data Availability Statement

The data that support the findings of this study are available from the corresponding author upon reasonable request.

Keywords

colorectal, gelatin, hydrogel, nanoindentation, photopolymerization

Received: May 21, 2023

Revised: July 22, 2023

Published online:

- [1] H. Mohammadi, E. Sahai, *Nat. Cell Biol.* **2018**, *20*, 766.
- [2] D. A. C. Walma, K. M. Yamada, *Development* **2020**, *147*, dev175596.
- [3] C. Bonnans, J. Chou, Z. Werb, *Nat. Rev. Mol. Cell Biol.* **2014**, *15*, 786.
- [4] A. Z. Sahan, M. Baday, C. B. Patel, *Gels* **2022**, *8*, 496.
- [5] J. Sievers, V. Mahajan, P. B. Welzel, C. Werner, A. Taubenberger, *Adv. Healthcare Mater.* **2023**, *12*, 2202514.
- [6] A. Singh, N. Dalal, P. Tayalia, *Biomed. Mater.* **2023**, *18*, 025010.
- [7] A. I. Van Den Bulcke, B. Bogdanov, N. De Rooze, E. H. Schacht, M. Cornelissen, H. Berghmans, *Biomacromolecules* **2000**, *1*, 31.
- [8] N. Celikkin, S. Mastrogiamco, J. Jaroszewicz, X. F. Walboomers, W. Swieszkowski, *J. Biomed. Mater. Res. A* **2018**, *106*, 201.
- [9] C. Kilic Bektas, V. Hasirci, *Biomater. Sci.* **2020**, *8*, 438.
- [10] S. Zigon-Branc, M. Markovic, J. Van Hoorick, S. Van Vlierberghe, P. Dubruel, E. Zerobin, S. Baudis, A. Ovsianikov, *Tissue Eng. Part A* **2019**, *25*, 1369.
- [11] X. Zhao, Q. Lang, L. Yildirimer, Z. Y. Lin, W. Cui, N. Annabi, K. W. Ng, M. R. Dokmeci, A. M. Ghaemmaghami, A. Khademhosseini, *Adv. Healthcare Mater.* **2016**, *5*, 108.
- [12] E. Andrzejewska, in *Three-Dimensional Microfabrication Using Two-photon Polymerization*, (Ed: T. Baldacchini), William Andrew Publishing, Oxford, **2016**, Ch. 2.
- [13] J. Del Barrio, C. Sánchez-Somolinos, *Adv. Opt. Mater.* **2019**, *7*, 1900598.
- [14] S. K. Seidlits, Z. Z. Khaing, R. R. Petersen, J. D. Nickels, J. E. Vanscoy, J. B. Shear, C. E. Schmidt, *Biomaterials* **2010**, *31*, 3930.
- [15] A. J. Berger, K. M. Linsmeier, P. K. Kreeger, K. S. Masters, *Biomaterials* **2017**, *141*, 125.
- [16] R. Pamplona, S. González-Lana, P. Romero, I. Ochoa, R. Martín-Rapún, C. Sánchez-Somolinos, *ACS Appl Polym Mater* **2023**, *5*, 1487.
- [17] M. A. Daniele, A. A. Adams, J. Naciri, S. H. North, F. S. Ligler, *Biomaterials* **2014**, *35*, 1845.
- [18] N. F. Haruna, J. Huang, *J. Cytol. Tissue Biol.* **2020**, *7*, 030.
- [19] D. Gupta, J. W. Santoso, M. L. McCain, *Bioengineering (Basel)* **2021**, *8*, 6.
- [20] M. Monfared, M. D. Nothling, D. Mawad, M. H. Stenzel, *Biomacromolecules* **2021**, *22*, 4295.
- [21] P. J. Price, *In Vitro Cell. Dev. Biol. - Anim.* **2017**, *53*, 673.
- [22] T. Ackermann, S. Tardito, *Trends Cancer* **2019**, *5*, 329.
- [23] L. Mauri, G. Boccardi, G. Torri, M. Karfunkle, E. Macchi, L. Muzi, D. Keire, M. Guerrini, *J. Pharm. Biomed. Anal.* **2017**, *136*, 92.
- [24] I. D. Gaudet, D. I. Shreiber, *Biointerphases* **2012**, *7*, 25.
- [25] C. Willems, M.-L. Trutschel, V. Mazaikina, J. Strätz, K. Mäder, S. Fischer, T. Groth, *Macromol. Biosci.* **2021**, *21*, 2100098.
- [26] S. Kawano, M. Kojima, Y. Higuchi, M. Sugimoto, K. Ikeda, N. Sakuyama, S. Takahashi, R. Hayashi, A. Ochiai, N. Saito, *Cancer Sci.* **2015**, *106*, 1232.
- [27] R. Schrieber, H. Gareis, *Gelatine Handbook: Theory and Industrial Practice*, John Wiley & Sons, Weinheim, Chichester, **2007**.
- [28] J. Van Hoorick, P. Gruber, M. Markovic, M. Tromayer, J. Van Erps, H. Thienpont, R. Liska, A. Ovsianikov, P. Dubruel, S. Van Vlierberghe, *Biomacromolecules* **2017**, *18*, 3260.
- [29] K. Yue, G. Trujillo-de Santiago, M. M. Alvarez, A. Tamayol, N. Annabi, A. Khademhosseini, *Biomaterials* **2015**, *73*, 254.
- [30] M. Sun, X. Sun, Z. Wang, S. Guo, G. Yu, H. Yang, *Polymers* **2018**, *10*, 1290.
- [31] S. Xiao, T. Zhao, J. Wang, C. Wang, J. Du, L. Ying, J. Lin, C. Zhang, W. Hu, L. Wang, K. Xu, *Stem Cell Rev. Rep.* **2019**, *15*, 664.
- [32] C.-Y. Lin, C.-H. Lee, C.-C. Huang, S.-T. Lee, H.-R. Guo, S.-B. Su, C.-Y. Lin, *World J. Gastroenterol.* **2015**, *21*, 2047.
- [33] G. Cui, Y. Huang, W. Feng, Y. Yao, H. Zhou, X. Li, H. Gong, J. Liu, Y. Luo, Y. Sun, M. Zhang, Y. Luo, T. Zhang, *J. Gastrointest. Oncol.* **2020**, *11*, 1164.
- [34] M. L. Oyen, *Int. Mater. Rev.* **2014**, *59*, 44.
- [35] T. Billiet, B. V. Gasse, E. Gevaert, M. Cornelissen, J. C. Martins, P. Dubruel, *Macromol. Biosci.* **2013**, *13*, 1531.
- [36] S. Van Vlierberghe, B. Fritzing, J. C. Martins, P. Dubruel, *Appl. Spectrosc.* **2010**, *64*, 1176.
- [37] C. Claaßen, M. H. Claaßen, V. Truffault, L. Sewald, G. E. M. Tovar, K. Borchers, A. Southan, *Biomacromolecules* **2018**, *19*, 42.
- [38] Y.-K. Wu, Y.-K. Tu, J. Yu, N.-C. Cheng, *Sci. Rep.* **2020**, *10*, 104.
- [39] D. Njus, P. M. Kelley, Y.-J. Tu, H. B. Schlegel, *Free Radic. Biol. Med.* **2020**, *159*, 37.
- [40] R. L. Dimarco, D. R. Hunt, R. E. Dewi, S. C. Heilshorn, *Biomaterials* **2017**, *129*, 152.
- [41] L. Elomaa, E. Keshi, I. M. Sauer, M. Weinhardt, *Mater. Sci. Eng.: C* **2020**, *112*, 110958.
- [42] C. Te Chiang, R. Lau, A. Ghaffarizadeh, M. Brovold, D. Vyas, E. F. Juárez, A. Atala, D. B. Agus, S. Soker, P. Macklin, D. Ruderman, S. M. Mumenthaler, *GigaScience* **2021**, *10*, giab026.
- [43] Y. Sambuy, I. De Angelis, G. Ranaldi, M. L. Scarino, A. Stammati, F. Zucco, *Cell Biol. Toxicol.* **2005**, *21*, 1.
- [44] X. Gong, K. L. Mills, *Sci. Rep.* **2018**, *8*, 3849.